A&A 374, L21–L24 (2001)
DOI: 10.1051/0004-6361:20010872


Astronomy & Astrophysics

Letter to the Editor

# The size of penumbral fine structure

P. Sütterlin*

Sterrenkundig Instituut Utrecht, Postbus 80 000, 3507 TA Utrecht, The Netherlands

Received 21 May 2001 / Accepted 19 June 2001

**Abstract.** I present power spectra of penumbral and granular intensity variations from a speckle-restored $G$-band image sequence of sunspot NOAA 9407 taken on April 1, 2001 with the Dutch Open Telescope on La Palma. I compare spatial power spectra of the sunspot penumbra with spatial power spectra from granulation with and without filigree. Relative to the granular power distribution, the penumbral power spectrum is enhanced over a wide range in spatial frequency peaking at $0\farcs35$. For smaller scales, the penumbral power distribution closely resembles that of the granular intensity variations. In contrast, the power spectrum of granulation with filigree exhibits increased power down to the resolution limit of $0\farcs22$, indicating the presence of unresolved magnetic elements.

**Key words.** Sun: magnetic fields – sunspots

## 1. Introduction

Sunspot penumbrae remain a source of many open questions in solar physics (e.g. Thomas & Weiss 1992). While it is generally accepted that the structuring of a penumbra into more or less radially directed dark and bright filaments is dominated by magnetic fields, the composition of the penumbral filaments remains controversial. Do they form a flat layer on top of the granulation, or do they constitute a thick structure extending down in the sun? How large are the individual elements? While the former question requires theoretical modeling (see e.g. Jahn 1997), the latter issue can benefit from high angular resolution observations. I address the second question here.

The typical size of a penumbral filament is $0\farcs35 \times 0\farcs5 - 2''$ (Sobotka 1997), but there are measurements that go down to $0\farcs11$ (Stachnik et al. 1983). The numerical model of Schlichenmaier et al. (1998) uses flux tubes of 50 km diameter. A model of Sánchez Almeida (1998) postulates that the whole penumbra consists of tiny fibrils as small as 1–10 km. Although the fibrils would be too narrow to be observed individually (being much smaller than the photon mean free path), such a micro-structured magnetic atmosphere (MISMA) allows Sánchez to explain the broadband circular polarization characteristics of penumbrae (but see Martínez Pillet 2000 and the comments in Sánchez Almeida 2001 and Martínez Pillet 2001).

Sánchez Almeida & Bonet (1998) analyzed spatial power spectra of penumbral intensity variations and claim that these follow closely the combined modulation transfer function (MTF) of the telescope and atmosphere, implying a basically flat power spectrum of the intrinsic intensity variations. This conclusion is somewhat ambiguous because the MTF for the atmospheric disturbances could not be measured from the data but was extrapolated from other sources and became uncertain below $0\farcs4$. However, the authors point out that this ambiguity may be removed by methods such as speckle image reconstruction that deliver the MTF down to the resolution limit of the telescope. The Dutch Open Telescope (DOT) at the Observatorio del Roque de Los Muchachos on La Palma (Hammerschlag & Bettonvil 1998) represents a new solar telescope which indeed employs speckle reconstruction as its standard observing technique. Under standard seeing conditions the speckle image processing delivers the theoretical resolution limit of $0\farcs2$ at 4300 Å (aperture 45 cm). In this analysis I use DOT speckle observations of a sunspot penumbra to test whether the spatial fine structure is resolved at this limit.

## 2. Observations

A one-hour time sequence of $G$-band images (4305±5 Å) of sunspot NOAA 9407 (radius $\sim 19''$) was obtained on April 1, 2001 with the DOT using the new CCD camera (10 bit, 1296×1030 px, see Rutten et al. 2000). The data were taken in bursts of 100 images at a rate of 6 fps to permit the speckle reconstruction described below. In total, 120 such bursts were collected at a cadence of 30 s during 9:00–10:00 UT. The seeing conditions were quite good, with Fried parameter $r_0 = 7-10$ cm. The image scale in the secondary focus of the DOT was set to $0\farcs071$ per pixel to allow sampling up to the resolution limit ($0\farcs2$) also along diagonals.

* e-mail: P.Suetterlin@astro.uu.nl

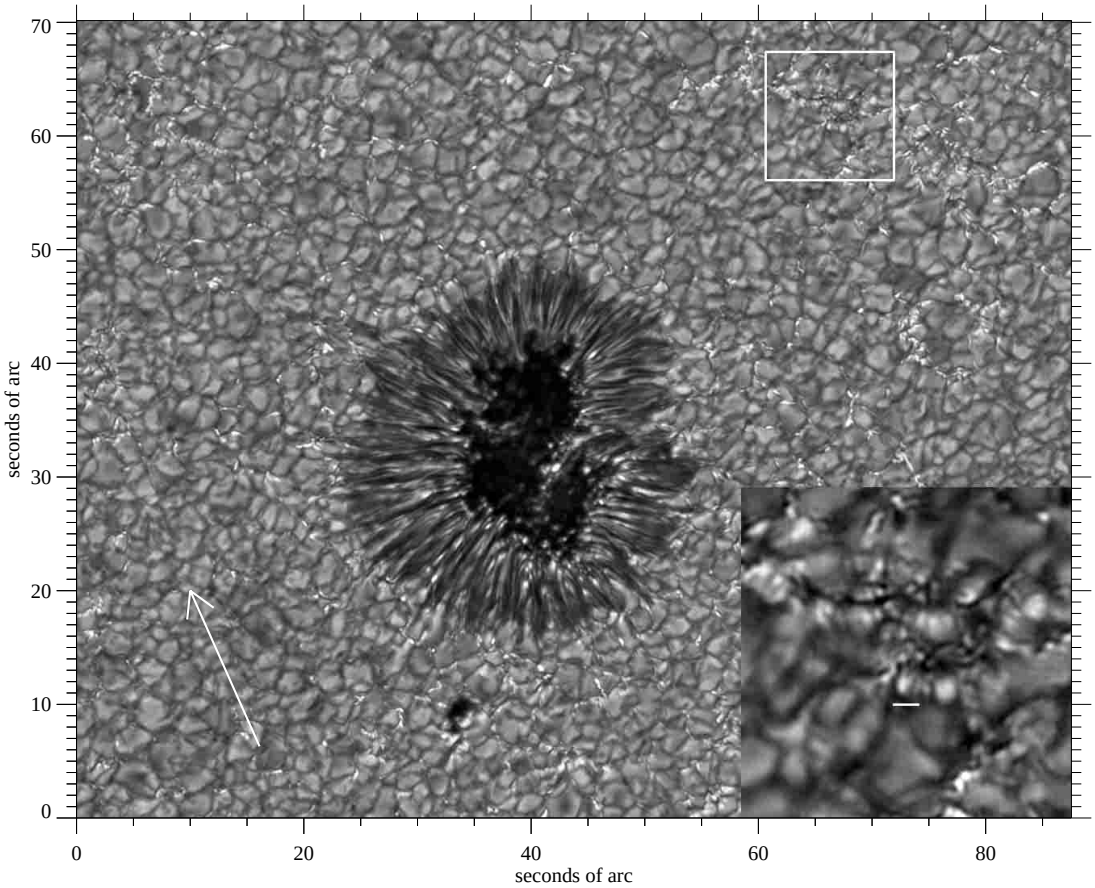


**Fig. 1.** Example of a speckle-reconstructed image of NOAA 9407. The position of the spot was N11 E21 ($\mu = 0.89$), the arrow marks the direction towards disk center. The inset in the lower right is an enlargement of the granular area containing filigree that is marked in the main image. The dash measures 1 arcsec.

## 3. Data reduction

### 3.1. Speckle masking

The first step in the data reduction was speckle reconstruction through treating the individual bursts with the speckle masking algorithm (Weigelt & Wirnitzer 1983; von der Lühe 1984). This method requires a burst of many frames that show the same object with varying atmospheric distortion in order to sample the seeing. The frames of one such burst are combined using a model for the atmospheric influence (Korff 1973) and a statistical approach for summing the Fourier phases in a bispectrum (Lohmann et al. 1983) into a single image that is free of atmospheric influence and is also corrected for the theoretical modulation transfer function (MTF) of the telescope, based on the actual aperture including all secondary-focus obstructions but without optical aberrations. The restriction is that the frames in each burst have to be collected before the object changes. For the solar photosphere this implies that the burst must be completed within the time span in which a solar disturbance crosses a telescope resolution element. Permitting horizontal velocities of a few km/s, the size of the pixel size, which corresponds to 50 km on the sun, limits the burst duration to about 15 s. At 6 fps frame rate this allows bursts of 100 frames. At reasonable seeing conditions (Fried parameter $r_0 \geq 6$ cm) this number suffices to obtain reconstructions close to the diffraction limit. At yet better seeing ($r_0 \geq 10$ cm) the reconstruction is complete, revealing structures down to the resolution limit of the optic. The reconstruction also quantifies the value of the Fried parameter $r_0$ during each burst.

Burst-mode image acquisition and subsequent speckle reconstruction have been selected to be the standard observing mode of the DOT. Speckle-restored movies of this (and other) time sequences are available on the DOT website[1].

I selected the image with the highest Fried parameter $r_0$ in the sequence for further investigation. It is shown in Fig. 1 and it had $r_0 = 10$ cm. The inset at the lower right shows a magnification of an area containing filigree to demonstrate that the reconstruction reveals fine structure down to the telescope's diffraction limit.

### 3.2. Interference filtering

Close inspection of the data showed that an electronic interference in the read-out system of the CCD camera introduced spurious high frequency variations in the data.

[1] `http://dot.astro.uu.nl`

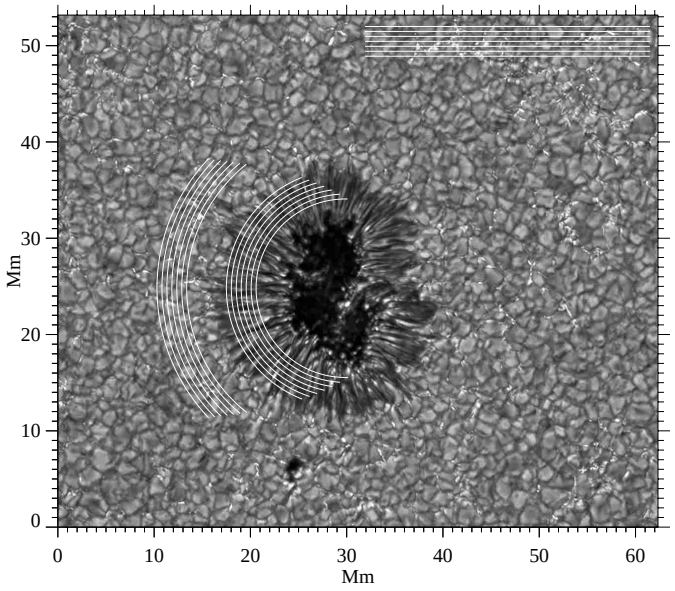


**Fig. 2.** Sunspot image after correction for geometrical distortion. The superimposed curves indicate the positions of the slices.

This signal is constrained to wave numbers higher than approximately $39\,\mathrm{Mm}^{-1}$. Therefore a low-pass filter with that cut-off was applied to the data, slightly reducing the actual resolution limit to 0.″22.

### 3.3. Geometrical corrections

The sun being spherical produces clinching of solar surface images along the radial direction by a factor $\mu = \cos\theta$, while the orthogonal direction remains unaffected (neglecting curvature and approximating solar polar coordinates by Cartesian ones). For the position of the spot (N11 E21) this correction factor is $\mu = 0.89$. The angle between north and the direction towards disk center is 156°. I computed the corresponding transformation matrix and regridded the image using cubic interpolation. The resulting rhomb was then clipped back to a rectangle, slightly reducing the field. Figure 2 shows the destretched spot. The pixel size of 0.″07 now covers the same geometrical size on the solar surface in both directions, i.e. 51.5 km.

### 3.4. Measuring power spectra

Penumbral filaments are radially oriented. In order to obtain information on their cross-sections one has to examine intensity variations along circular paths around the spot. Unfortunately, the spot is not circular and possesses some areas where the penumbra is irregular. I therefore used only partial circle paths and chose to use slices of constant length, so that the opening angle of the sector decreases with increasing radius. The positions of the selected slices are shown in Fig. 2. The intensity along each arc was interpolated from the image using a constant step width corresponding to 1 pixel, again using cubic interpolation. I used seven slices in the penumbra to evaluate spatial power spectra. Seven more arc-shaped slices are located in the relatively quiet sunspot moat for comparison with standard granulation behavior. Straight cuts that sample more active granulation were taken in a region that contains filigree (at the upper right of the spot).

An apodisation window was applied for the computation of the power spectra to remove the influence of non-periodic boundary conditions. I used a simple cosine falloff over the outer 10% of each segment. The data sampling is fine enough to fully cover the resolution of the telescope, so that there are no aliasing effects.

Polynomic interpolation of data before computing a power spectrum tends to produce spurious signals. This can be seen in Fig. 3: beyond the cut-off frequency of the telescope the power spectrum of the granulation with filigree, which was not interpolated on circular paths, drops down, while for the interpolated ones it stays at approximately $10^{-8}$. This artificial signal is however much smaller than the measured values and therefore does not influence the results.

## 4. Results

Figure 3 shows the power spectra along the selected slices, split between the three types of area. There are no distinctive differences between the different paths in each area type, so all power values are plotted with the same symbol. The diamonds are the averages over the different slices, with the solid curve a smoothed fit. Each plot also repeats the fits from the other two panels to facilitate comparisons.

None of the three power spectra show evidence of constancy with frequency but they all exhibit a steady decline out to the resolution limit (0.″22) without apparent flattening. The shape and slope of the power spectrum of granulation without filigree match the result of previous investigations that also used image reconstruction (von der Lühe & Dunn 1987; Wilken et al. 1997; Sánchez Cuberes et al. 2000).

Compared to the power spectrum of the quiet granulation, the penumbral power spectrum shows a region of enhanced power in the range between 13 and 32 $\mathrm{Mm}^{-1}$ with a broad maximum at 25 $\mathrm{Mm}^{-1}$, corresponding to a structure size of 0.″35. This value coincides with the width given by Sobotka (1997) as the typical size of penumbral filaments. For higher wavenumbers ($k > 32\,\mathrm{Mm}^{-1}$) the power spectra of the penumbral filaments and the quiet granulation are identical.

One might argue that the steady decline is due to incomplete restoration or imperfections in the numerical treatment. However, the active granulation containing filigree deviates from this behavior and exhibits clearly increased power up to 38 $\mathrm{Mm}^{-1}$ where the low pass filter sets in. This proves that the reconstruction indeed does uncover structures out to the resolution limit, if they are present. Assuming that this excess of power continues towards higher wave-numbers one can infer that the size of

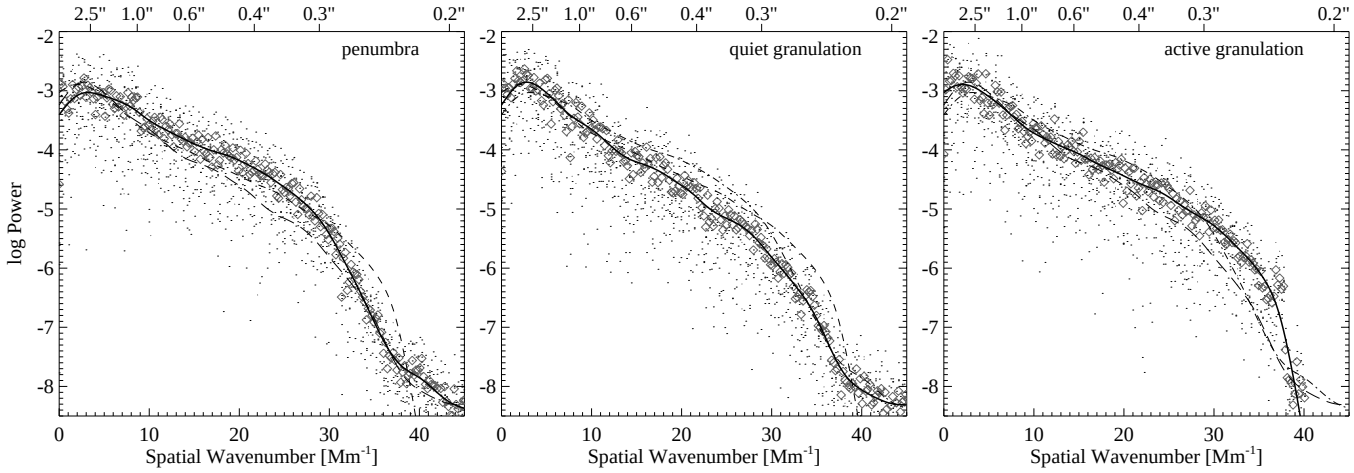


**Fig. 3.** Power spectra of the selected slices through penumbra (left), quiet (middle), and active granulation (right). Dots: power spectra per slice; diamonds: average. The thick curve is a fit to the average values, the dashed curves show the power distribution of the other two categories.

the filigree is below the resolution limit. This suggestion is strengthened by inspecting single bright points in the inset in Fig. 1: these are circular and closely resemble the Airy function of the telescope for point objects.

## 5. Conclusions

Our speckle-restored high-resolution data do not agree with the notion of intrinsically flat spatial power spectra. The penumbral enhancement of spatial power over 0.″3–0.″6 over granular power behavior supports the earlier result that penumbral filaments have preferred widths of about 250 km. Contrary to Sánchez Almeida & Bonet (1998) who used a broad band continuum filter, these data were taken in the *G*-band and might therefore sample the atmosphere in a somewhat different height. The resulting power spectra may differ slightly between continuum and *G*-band, but it is unlikely that they do so in basic properties.

It should also be pointed out that inspection of the power spectra presented by Sánchez Almeida & Bonet (1998) also shows an indication of enhanced power around 0.″35, however the authors attribute that to the MTF that is very uncertain below 0.″4. The results presented here do not suffer from this uncertainty, as the speckle reconstruction delivers the true MTF of telescope and atmosphere down to the resolution limit of 0.″22.

This result does neither confirm nor disprove the MISMA concept of Sánchez Almeida (1998), but the question that arises is why, if the basic structures in the penumbra have MISMA widths of a few km only each, they build conglomerates preferentially at 200–500 km cross-cut scales.

*Acknowledgements.* This research is funded by the European Solar Magnetometry Network (ESMN) under EC-TMR contract ERBFMRXCT98019. The DOT project is funded by Utrecht University, the Netherlands Graduate School for Astronomy NOVA and the Netherlands Organization for Scientific Research NWO. The new DOT data acquisition system was built by the Instrumentele Groep Fysica IGF at Utrecht. R. H. Hammerschlag and F. C. M. Bettonvil assisted in the observing. I acknowledge helpful comments from R. J. Rutten and the referee.

## References

Hammerschlag, R. H., & Bettonvil, F. C. M. 1998, New Astron. Rev., 42, 485
Jahn, K. 1997, in 1st Advances in Solar Physics Euroconference, Advances in Physics of Sunspots, ASP Conf. Ser., 118, 122
Korff, D. 1973, J. Opt. Soc. Am., 63, 971
Lohmann, A. W., Weigelt, G., & Wirnitzer, B. 1983, Appl. Opt., 22, 4028
Martínez Pillet, V. 2000, A&A, 361, 734
Martínez Pillet, V. 2001, A&A, 369, 644
Rutten, R. J., Hammerschlag, R. H., Bettonvil, F. M., & Sütterlin, P. 2000, in AAS/Solar Physics Division Meeting, vol. 32, 02107
Sánchez Almeida, J. 2001, A&A, 369, 643
Sánchez Almeida, J. 1998, ApJ, 497, 967
Sánchez Almeida, J., & Bonet, J. A. 1998, ApJ, 505, 1010
Sánchez Cuberes, M., Bonet, J. A., Vázquez, M., & Wittmann, A. D. 2000, ApJ, 538, 940
Schlichenmaier, R., Jahn, K., & Schmidt, H. U. 1998, A&A, 337, 897
Sobotka, M. 1997, in 1st Advances in Solar Physics Euroconference, Advances in Physics of Sunspots, ASP Conf. Ser., 118, 155
Stachnik, R. V., Nisenson, P., & Noyes, R. W. 1983, ApJ, 271, L37
Thomas, J. H., & Weiss, N. O. (ed.) 1992, Sunspots: Theory and observations, Proceedings of the NATO Advanced Research Workshop on the Theory of Sunspots, Cambridge, United Kingdom, Sept. 22–27, 1991
von der Lühe, O. 1984, J. Opt. Soc. Am. A, 1, 510
von der Lühe, O., & Dunn, R. B. 1987, A&A, 177, 265
Weigelt, G., & Wirnitzer, B. 1983, Optics Lett., 8, 389
Wilken, V., de Boer, C. R., Denker, C., & Kneer, F. 1997, A&A, 325, 819